The EMBO Journal (2009) 28, 1043–1054 | © 2009 European Molecular Biology Organization | Some Rights Reserved 0261-4189/09
www.embojournal.org

THE EMBO JOURNAL

EMBO open

Acid sphingomyelinase activity triggers microparticle release from glial cells

Fabio Bianco[1,2,9], Cristiana Perrotta[3,9], Luisa Novellino[1,9], Maura Francolini[1], Loredana Riganti[1], Elisabetta Menna[1], Laura Saglietti[1], Edward H Schuchman[4], Roberto Furlan[5], Emilio Clementi[6,7], Michela Matteoli[1,8] and Claudia Verderio[1,*]

[1]CNR Institute of Neuroscience and Department of Medical Pharmacology, University of Milano, Milano, Italy, [2]NeuroZone srl, Milano, Italy, [3]Hospital of Luigi Sacco, Milano, Italy, [4]Department of Genetics and Genomic Science, Mount Sinai School of Medicine, New York, NY, USA, [5]Clinical Neuroimmunology Unit, Institute of Experimental Neurology, S Raffaele Scientific Instute, Milano, Italy, [6]Medea Science Institute, Bosisio Parini, Italy, [7]Department of Preclinical Science, LITA-Vialba University of Milano, Milano, Italy and [8]Fondazione Don Gnocchi, Milano, Italy

We have earlier shown that microglia, the immune cells of the CNS, release microparticles from cell plasma membrane after ATP stimulation. These vesicles contain and release IL-1β, a crucial cytokine in CNS inflammatory events. In this study, we show that microparticles are also released by astrocytes and we get insights into the mechanism of their shedding. We show that, on activation of the ATP receptor $P2X_7$, microparticle shedding is associated with rapid activation of acid sphingomyelinase, which moves to plasma membrane outer leaflet. ATP-induced shedding and IL-1β release are markedly reduced by the inhibition of acid sphingomyelinase, and completely blocked in glial cultures from acid sphingomyelinase knockout mice. We also show that p38 MAPK cascade is relevant for the whole process, as specific kinase inhibitors strongly reduce acid sphingomyelinase activation, microparticle shedding and IL-1β release. Our results represent the first demonstration that activation of acid sphingomyelinase is necessary and sufficient for microparticle release from glial cells and define key molecular effectors of microparticle formation and IL-1β release, thus, opening new strategies for the treatment of neuroinflammatory diseases.

The EMBO Journal (2009) **28,** 1043–1054. doi:10.1038/emboj.2009.45; Published online 19 March 2009
Subject Categories: signal transduction; neuroscience
Keywords: A-SMase; glia; IL-1β; microparticles; $P2X_7$

*Corresponding author. CNR Institute of Neuroscience, Department of Medical Pharmacology, Via Vanvitelli 32, 20129 Milano, Italy.
Tel.: +39 02 50317097; Fax: +39 02 7490574;
E-mail: c.verderio@in.cnr.it
[9]These authors equally contributed to this work

Received: 21 November 2008; accepted: 29 January 2009; published online: 19 March 2009

Introduction

Cells communicate and exchange information by different secreting mechanisms. Among these, extracellular vesicles (exosomes and plasma membrane (PM)-derived microparticles, MPs) are gaining increasing attention as efficient vehicles for the release of signalling molecules. Exosomes are secreted as a result of multivesicular bodies (MVB) fusion with the PM, represent a population of vesicles homogenous in size and shape (40–80 nm). PM-derived MPs represent instead a heterogeneous population of vesicles larger than exosomes (100 nm–1 μm), which bud directly from the PM of healthy cells and contain cytoskeleton and ER elements (Ratajczak *et al*, 2006). MPs have high levels of phosphatidylserine (PS) exposed to the outer membrane (MacKenzie *et al*, 2001), whereas exosomes have lower PS exposed to the outer membrane leaflet, depending on cell type and stimuli, but over express tetraspanin superfamily of proteins, including CD63 (Heijnen *et al*, 1999; Théry *et al*, 2001; Morelli *et al*, 2004; Simpson *et al*, 2008). Both exosomes and MPs control fundamental cellular responses, such as intercellular signalling and immune reactions (Ratajczak *et al*, 2006; Simpson *et al*, 2008). Release of exosomes has received only limited attention in the CNS (Potolicchio *et al*, 2005; Fauré *et al*, 2006; Schiera *et al*, 2007; Taylor *et al*, 2007), where these organelles might mediate cell-to-cell transfer of proteins, lipid components or mRNAs, as already demonstrated outside the CNS (Smalheiser, 2007). So far, regarding MP release in the CNS, there is only one study (Bianco *et al*, 2005) showing that microglia release MPs on ATP stimulation. Microglial MPs store and release the inflammatory cytokine IL-1β (Bianco *et al*, 2005), a leaderless protein that is not liberated through the default Golgi secreting pathway. Pro-IL-1β is present in MPs 10 min after microglia exposure to ATP, and it is then released into the medium (Bianco *et al*, 2005). Besides MPs (MacKenzie *et al*, 2001; Bianco *et al*, 2005), different pathways of secretion mediate IL-1β release in distinct cell types. Among these, release of exosomes (Qu *et al*, 2007), exocytose of secretory lysosomes (Andrei *et al*, 1999), and direct efflux through PM transporters (Marty *et al*, 2005). In microglia, MP shedding is rapidly induced by the activation of the ionotropic ATP receptor $P2X_7$ ($P2X_7R$). Activation of the receptor can occur at the site of lesion by ATP leaking from degenerating cells (Ferrari *et al*, 1997) or, distantly from the lesion, through propagation of ATP-mediated Ca^{2+} wave among astrocytes, a process that has a function in pathological signalling events (Nedergaard *et al*, 2003). The $P2X_7R$ is a ligand-gated ATP receptor, which, besides acting as a channel and pore, is known to be coupled to several downstream effectors and protein kinases (Duan and Neary, 2006). $P2X_7R$-mediated MP shedding is preceded by exposure of PS at the cell surface, loss of PM asymmetry and formation of

membrane protrusions, described in the literature as blebs. Intracellular signalling events required for MP release involve multiple pathways initiated by agonist occupancy of the $P2X_7R$, including activation of ROCK and p38 MAP kinase (p38 MAPK) (Morelli *et al*, 2003; Verhoef *et al*, 2003), similarly to apoptotic blebbing (Coleman *et al*, 2001). However, $P2X_7R$-induced morphological changes leading to MP release are reversible and not linked to apoptotic cell death (MacKenzie *et al*, 2001; Verhoef *et al*, 2003). How signalling by $P2X_7R$ leads to membrane blebbing is not known. In particular, nothing is known about $P2X_7R$-induced alterations of the biophysical properties of the PM, which together with actin-cytoskeleton reorganisation are a prerequisite for membrane blebbing and vesiculation at the surface of healthy cells. Blebbing and vesiculation in response to apoptotic stimuli, during the final stages of cell death, depend on breakdown of sphingomyelin (SM), a phospholipid abundant in the outer leaflet of the PM. SM has a high affinity for cholesterol and both lipids are major determinants of membrane fluidity and structural integrity of the PM (Simons and Ikonen, 1997). SM hydrolysis, catalysed by the enzyme family of sphingomyelinases (SMases), results in increased efflux of cholesterol and increased membrane fluidity (Slotte *et al*, 1989; Neufeld *et al*, 1996), thus inducing membrane destabilisation and facilitating membrane blebbing and MP shedding (Van Blitterswijk *et al*, 1982; Chang *et al*, 1993; Tepper *et al*, 2000). Therefore, we investigated the role of SMases in $P2X_7R$-triggered blebbing and found that receptor stimulation leads to the activation of a specific SMase, acid SMase (A-SMase) with rapid SM hydrolysis and MP formation. We also showed the obligatory role of A-SMase in the short term, non-apoptotic process of MP production and showed that A-SMase acts as a $P2X_7R$ effector, downstream of p38 phosphorylation, thus, defining the role of p38 activation in membrane blebbing.

Results

$P2X_7$-dependent MP shedding from astrocytes

We have earlier shown that stimulation of $P2X_7R$ by ATP or the selective agonist Benzoyl-ATP (BzATP) induces MP shedding from microglia cell surface (Bianco *et al*, 2005). In this study, we show that MP shedding occurs also in astrocytes. To study the dynamics of MP formation, we briefly labelled the lipid bilayers of primary cortical astrocytes or glial cell lines with the fluorescent styryl dye FM1–43 or with the fluorophore-conjugated phosphocholine compound NBD C_6-HPC and observed the cells by time-lapse fluorescence video microscopy. By this approach, we observed not only the formation (Figure 1A) but also the shedding from the PM of variably sized vesicles on 100 μM BzATP exposure (Figure 1B and C; Supplementary Movie). To quantify the shedding process, supernatant of glial cells exposed to BzATP for 20 min were pelleted at 10 000 *g*, to separate MPs as pellet (Heijnen *et al*, 1999). Fluorescence of pelleted MPs was then quantified by spectrophotometric analysis (Supplementary Figure 1; see also Figure 2). Several perturbants were tested for their effects on MP shedding, including the $P2X_7$ antagonists Brilliant Blue G (100 nM) and KN-62 (10 μM), the $P2X_{2,4}$ antagonist TNP-ATP (3 nM), the Rho-effector kinase inhibitor Y-27632 dihydrochloride (100 μM) and the actin polymerisation inhibitor cytochalasin D (2 μg/ml), as well as perturbants of Ca^{2+} homeostasis, such as the Ca^{2+} chelators EDTA (500 μM) and BAPTA (30 μM) and the Ca^{2+} ionophore ionomycin (10 μM). Phorbol ester PMA (1 μM) was also used as positive control for the shedding process. The results of this analysis indicated that BzATP-induced MP shedding in astrocytes requires both $P2X_7R$ activation and cytoskeleton reorganisation, and it is dependent on both extracellular and cytoplasmic Ca^{2+} (Figure 1D and E).

Time course analysis of MP release in the medium indicated a gradual increase that is already significant 5 min after $P2X_7R$ stimulation reaching a plateau after 20 min (Figure 1F). Consistent with these data, time-lapse video microscopy indicated that MP shedding starts in about 1 and 2 min after $P2X_7R$ activation and persists for several minutes in the continuous presence of the receptor agonist (not shown).

Biochemical and morphological characterisation of distinct types of vesicles released from glial cells

To define the nature of fluorescent MPs shed from the PM distinguishing them from exosomes, we analysed the size and molecular features of both extracellular vesicle populations, MPs and exosomes, released from glial cells under these conditions. To this aim, the supernatants of glial cells were subjected to differential centrifugation (Supplementary data) followed by negative staining electron microscopy, fluorescence microscopy and western blotting analysis. By this combined approach, we could analyse also small vesicles pinching off from the PM and exosomes that could not be sized at video microscopy resolution. Vesicles of distinct sizes were detected by negative staining electron microscopy in the P2 (1200 *g*), P3 (10 000 *g*) and P4 (110 000 *g*) pellets. The P4 pellet consisted of cup-shaped vesicles in the range of 30–80 nm, corresponding to exosome size, whereas the P3 and P2 pellets contained relatively larger vesicles, characterised by a mean diameter of 155 ± 6 and 426 ± 51 nm, respectively (Figure 2A). Similar results were obtained with N9 microglia (Supplementary Figure 2A). Given that PM-derived MPs, differently from exosomes, present high levels of PS exposed to the outer membrane, we used this information to further characterise P2–P4 populations. Vesicles present in P2, P3 and P4 pellets were imaged by fluorescence microscopy after incubation with NBD C_6-HPC (3 μM), to stain vesicle membrane, or with FITC-annexin V (4.2 μg/ml), indicative of the presence of PS on the outer membrane. We found that PS is exposed on the surface of P2 and P3 but not P4 vesicles, thus, suggesting that P2 and P3 MPs mainly derive from PM blebbing. Although optical resolution is approximately 200 nm, we excluded that the lack of annexin V signal in P4 vesicles was due to resolution limits, as P4 vesicles could be visualised, although not sized, when treated with NBD (Figure 2B; Supplementary Figure 2B). Indeed quantitative analysis of annexin V binding to vesicles by flow cytometry analysis (FACS) indicated the presence of PS on the outer membrane in 70% P2, 36% P3 but only 5% of P4 vesicles (Figure 2C). P2–P4 vesicles were also analysed by western blotting (Supplementary data; Figure 2D; Supplementary Figure 2D), and/or fluorescence microscopy (Figure 2B) for some PM and exosome markers, to further characterise the nature of P2–P4 vesicles. Typical exosome markers, such as CD63 and heat shock protein HSP70 were clearly found in the P4 pellet, identifying P4 vesicles as exosomes. Few CD63

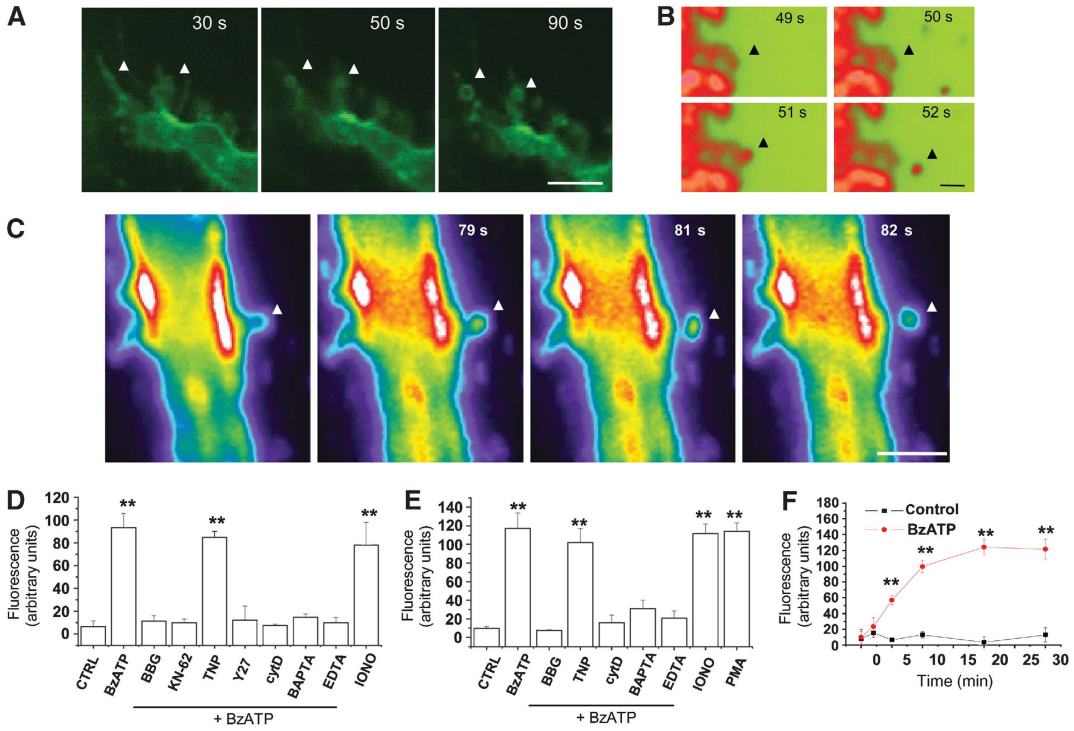

Figure 1 P2X$_7$-dependent MP shedding from glial cells. (**A–C**) Fluorescence images of FM1-43-labelled microglial N9 cells during 100 μM BzATP exposure (A, bar, 5 μm). Frames were taken at the indicated times after BzATP addition. BzATP treatment induces the formation of FM1-43-labelled vesicles along microglia philopodia (arrows). Fluorescence images of cortical astrocytes labelled with FM1-43 (B, bar, 1 μm) or NBD-labelled glioma cells (C, bar, 5 μm), showing the MP shedding from PM on BzATP exposure (see also Supplementary Movie). (**D**, **E**) The histograms show the spectrophotometric analysis of large fluorescent MPs pelletted at 10 000 *g* from supernatants of primary astrocytes (D) or N9 microglial cells (E) pre-labelled with FM1–43 and exposed to 100 μM BzATP for 20 min at 37°C. A significant reduction is observed in the amount of MPs released by cells exposed to BzATP after treatment with P2X$_7$R antagonists (BBG, KN-62, TNP), the Rho-effector kinase inhibitor Y-27632 (Y27), the actin polymerisation inhibitor cytochalasin D (cytD) or the Ca^{2+} chelators BAPTA and EDTA. Besides BzATP, ionomycin (IONO) and PMA were also able to stimulate MP release ($n=4$, $P<0.01$, ANOVA analysis, Dunnet's method). (**F**) Spectrophotometric analysis of MPs pelleted at 10 000 *g* from supernatants collected from FM1-43-labelled cortical astrocytes at different time points after BzATP stimulation, showing the kinetic of vesicle accumulation into the extracellular medium.

positive MPs were also present in P3 fraction (Figure 2B), although not detectable by western blotting (Figure 2D), probably due to the lower sensitivity of the antibody in immunoblotting than in immunocytochemistry. Conversely, P2 and P3 vesicles were positive for different PM markers including the cannabinoid receptor CB1, the glutamate transporter GLAST and Na^+/K^+ ATPase (Figure 2B and D; Supplementary Figure 2D). However, only CB1, among PM markers, was exclusively detected in P2 and P3 MPs (Supplementary Figure 2D). Both Na^+/K^+ ATPase and GLAST were indeed detectable also in the P4 exosome fraction (Figure 2B and D). This finding is consistent with the presence in exosomes of specific cell-surface proteins including integrins and cell adhesion molecules (Smalheiser, 2007).

We then evaluated which vesicle populations mediate IL-1β in astrocytes. Notably, western blotting of P2–P4 fractions for IL-1β indicated that the bulk of the pro-cytokine is present in PM-derived MPs pelleted in the P2 fraction. This analysis was carried out in both astrocytes (Figure 2D) and N9 microglial cells (Supplementary Figure 2D) exposed to BzATP for 15 min, a time point when about 80% of the released cytokine is detected inside MPs having PS on the membrane (Bianco *et al*, 2005). Overall, these results clearly indicate that PM-derived MPs and not exosomes mainly contributes to IL-1β release from glial cells.

A-SMase is enriched in glia-derived MPs

SMases catalyse the hydrolysis of SM into ceramide and phosphorylcholine thus controlling PM fluidity. Three forms of SMases with an optimal acidic, neutral, or alkaline pH have been described (Gulbins *et al*, 2000). Among SMases, A-SMase is activated rapidly on stimulation of various receptors, being recruited to the PM to mediate receptor-dependent signalling (Grassmé *et al*, 2001; Gulbins, 2003; Marchesini and Hannun, 2004). To investigate whether A-SMase may be involved in the P2X$_7$R-induced budding and release of MPs, we evaluated by western blotting the expression of A-SMase in MPs released from glial cells, isolated either by differential centrifugation (Figure 2D; Supplementary Figure 2D) or by binding to annexin V coated beads (Figure 2E), a method that allows selective enrichment of MPs exposing PS (Supplementary data). A significant enrichment of A-SMase in the PM-derived MPs was observed as compared with glial lysates.

A-SMase mediates P2X$_7$R-dependent MP shedding

To investigate the specific involvement of A-SMase in MP production, we directly measured A-SMase activity in microglia exposed for different time points to BzATP. Kinetic analysis of A-SMase activity revealed a peak of enzyme activity at 2 min after agonist addition (Figure 3A), indicating

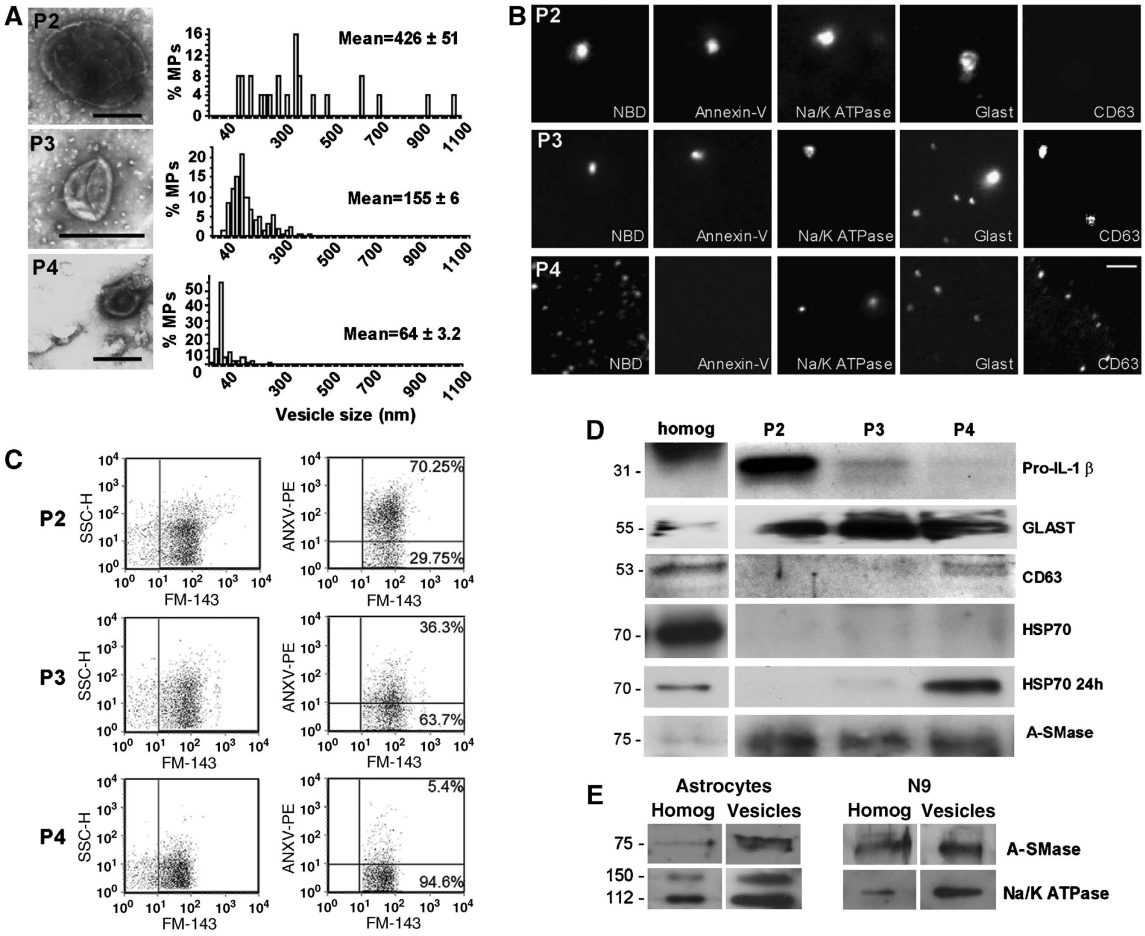

Figure 2 Morphological and biochemical characterisation of MPs released by cortical astrocytes. (**A**) Negative staining electron microscopy of P2 (bar, 300 nm), P3 (bar, 300 nm) and P4 (100 nm) vesicles pelleted from supernatant of astrocyte exposed to 100 μM BzATP for 20 min was carried out as described in Supplementary Figure 2. Number of analysed vesicles from three different preparations: $n = 50$, P2; $n = 161$, P3; $n = 184$, P4. (**B**) Fluorescence images of P2, P3 and P4 vesicles stained by NBD, annexin V, the exosome marker CD63 and Na^+/K^+ ATPase or GLAST, as PM markers. Bar, 5 μm. (**C**) FACS of astrocyte-derived P2, P3 and P4 vesicles labelled by annexin V-PE and NBD. (**D**) Western blotting of P2, P3 and P4 lysates obtained from medium conditioned for 30 min by 100 μM BzATP-treated astrocytes for IL-1β, A-SMase, membrane (GLAST) and exosome (CD63, HSP70) markers. Vesicle were loaded as described in Supplementary data. HSP70 staining is below ECL detectability in P4 vesicles 30 min after BzATP stimulation, but become clearly detectable in P4 vesicles on longer conditioning (24 h). For IL-1β blotting, vesicle fractions were obtained from supernatant of astrocytes exposed to BzATP for 15 min. (**E**) Immunoblot analysis of A-SMase and Na^+/K^+ ATPase in glial lysates and PM-derived MPs isolated by annexin V-coated beads (Supplementary data).

that the enzyme acts as a downstream effector of the receptor. Although A-SMase activation period is shorter than that of MP release (Figure 1F), it is plausible that increased generated ceramide has long-lasting effects on membrane fluidity required for $P2X_7$-dependent blebbing. Activation of A-SMase by $P2X_7R$ was accompanied by enzyme translocation to the PM outer leaflet, as shown by the increased A-SMase staining detected by FACS in intact cells (Figure 3B). A-SMase translocation to the PM outer leaflet on $P2X_7R$ activation was confirmed by biotynilation and western blotting experiments that revealed surface expression of the enzyme in cultured astrocytes during BzATP exposure (Figure 3C). Finally, A-SMase translocation was also suggested by movement of the enzyme from the exosomal fraction (P4) to PM-derived fractions, P2 and P3, on BzATP stimulation of microglial cells (Figure 3D). Interestingly, FACS analysis of intact P2, P3 and P4 vesicles for A-SMase revealed immunoreactivity for the enzyme in P2 and P3 but not in P4 pellet (Figure 3E). P4 vesicles were negative for outer A-SMase also under non-stimulating conditions (not shown), when these vesicles have highest luminal concentration of the enzyme (Figure 3D). These results, together with the presence of A-SMase in P4 fraction (Figures 2D and 3D), indicated both association of the enzyme to the outer leaflet of MPs and luminal localisation of A-SMase in exosomes. Furthermore, FACS experiments on intact vesicles doubled labelled with A-SMase and annexin V revealed that A-SMase immunoreactivity represented $87 \pm 5\%$ of total MPs exposing PS (not shown), indicating that the presence of the enzyme on MPs is instrumental for vesicle budding from PM.

To investigate whether A-SMase activity could facilitate formation of membrane protrusions and membrane vesiculation, microglia were exposed to exogenous recombinant SMase (r-SMase), which has an acid pH optima and displays little activity at neutral pH. Spectrophotometric quantification of the amount of MPs shed on exposure to r-SMase revealed that the enzyme is by itself sufficient to stimulate MP shedding. Similar results were obtained when astrocytes were exposed to bacterial SMase (b-SMase), thus indicating that ceramide generation is the key player in the shedding process

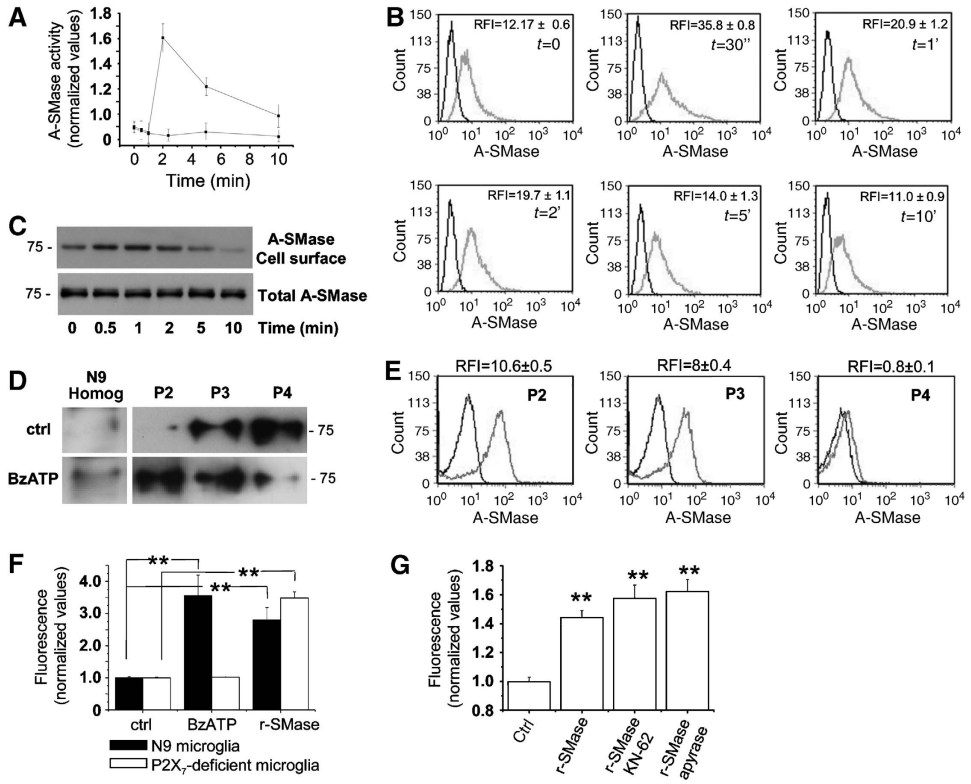

Figure 3 A-SMase is activated downstream of $P2X_7R$ stimulation. (**A**) Time course of A-SMase activation by 100 μM BzATP versus not stimulated cells as control, determined in cell lysates by measuring hydrolysis of sphingomyelin to phosphorylcholine at pH 5.5. Values are expressed as fold increases over basal A-SMase activity (1.12 ± 0.3 nmol/mg h^{-1}) conventionally indicated as 1 ($n = 3$). (**B**) A-SMase translocation onto the PM on $P2X_7R$ stimulation as determined by FACS analysis of intact N9 microglial cells. The relative fluorescence intensity (RFI) was calculated as ratio of sample mean fluorescence over negative control mean fluorescence. The RFI values reported in the panels are the mean ± s.e.m. measured in the three experiments. The results shown are from one out of three experiments. (**C**) Surface exposure of A-SMase on $P2X_7R$ stimulation, as detected by western blotting of biotinylated PM proteins with the A-SMase antibody. (**D**) Western blot analysis for A-SMase of P2, P3 and P4 vesicles accumulated in the supernatant of microglia cells under basal conditions or on stimulation with 100 μM BzATP for 30 min. (**E**) FACS analysis of intact P2, P3 and P4 vesicles for surface A-SMase, showing most of association of the enzyme to the outer leaflet of P2 and P3 MPs. (**F**) Spectrophotometric analysis of fluorescent MPs present in total supernatants collected from either FM1-43-labelled N9 microglial cells (black bars) or FM1-43-labelled N9 microglial clone, not expressing the $P2X_7R$ (white bars), 20 min after A-SMase (2 U/ml) or BzATP (100 μM) addition. (**G**) Quantitative analysis of FM1-43-labelled vesicles in the total supernatants of microglial cells exposed to exogenous A-SMase in the presence/absence of the $P2X_7R$ antagonist KN-62 or the ATP degrading enzyme apyrase.

(Figure 4D). Consistent with the activation of the enzyme downstream of $P2X_7R$, cell exposure to r-SMase also triggered MP shedding either in a $P2X_7$-deficient microglial cell clone (Figure 3F) or when $P2X_7R$ activation was prevented by specific antagonists, such as KN-62 (Figure 3G).

To directly prove the involvement of endogenous A-SMase in MP shedding, we then evaluated the effects of the A-SMase inhibitor imipramine (10 μM) on the amount of MPs. A clear inhibition of MP shedding from astrocytes (Figure 4C) and microglia (Supplementary Figure 3A) was detected with imipramine. No inhibitory effect was instead observed in cultures treated with inhibitors of neutral SMase (N-SMase) such as manumicyn (1 μM) or GW4869 (5 μM), which has been recently described to control exosome release (Trajkovic *et al*, 2008). Given that imipramine is not very specific for A-SMase and can interfere with other enzyme activities, the role of A-SMase in vesicle shedding was also proven in astrocyte cultures established from A-SMase heterozygous or knockout (KO) mice (Figure 4A and B). MP shedding was completely abolished in astrocytes from A-SMase KO and significantly reduced in astrocytes from heterozygous mice as compared with wild-type cultures (Figure 4D). Addition of r- or b-SMase efficiently induced MP shedding in KO astrocytes, as well as in heterozygous cultures, further indicating that SMase activity is sufficient to induce release of PM-derived MPs.

A-SMase activity mediates $P2X_7$-dependent IL-1β release

We then examined whether pharmacological inhibition of A-SMase activity or genetic deficiency of A-SMase could affect IL-1β release from either microglia or cortical astrocytes, which also release the cytokine on BzATP stimulation (Bianco *et al*, unpublished data). ELISA of IL-1β levels in the supernatants from cells pre-treated with imipramine indicated a strong reduction of cytokine release (Figure 4E; Supplementary Figure 3B). Furthermore, IL-1β release was completely abolished or strongly reduced in astrocyte cultures prepared from A-SMase KO or heterozygous mice, respectively (Figure 4F). Although an IL-1β expression reduction of about 50% was detected by optical density analysis in astrocyte homogenates from A-SMase KO cultures as compared with controls (Figure 4B for an example of western blotting), exposure to r- or b-SMases partially restored BzATP-induced IL-1β release (Figure 4F), thus,

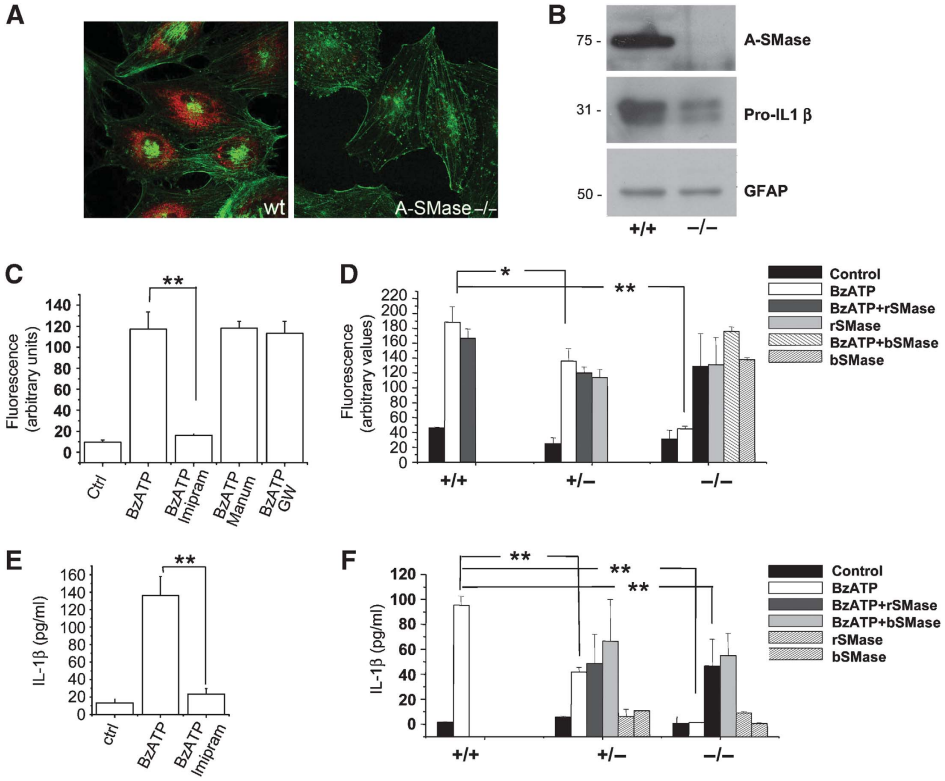

Figure 4 Endogenous A-SMase mediates $P2X_7$-induced vesicle shedding and IL-1β release. (**A**) Confocal images of cultured astrocytes from wt and A-SMase KO mice, stained for A-SMase (red) and falloidin (green) to show the specificity of A-SMase Ab. (**B**) Western blotting for A-SMase, IL-1β and GFAP carried out on wild type and A-SMase KO astrocyte lysates primed with LPS. (**C**) Quantitative analysis of 10 000 *g* pelleted MPs from FM1-43-labelled astrocytes pre-treated or not with the A-SMase inhibitor imipramine or the neutral SMase (N-SMase) inhibitors manumycin or GW4869, and then exposed to 100 μM BzATP for 20 min (n of experimental sessions = 2, $P<0.01$, ANOVA analysis, Scheffe's method). (**D**) Spectrophotometric analysis of MPs present in the total supernatants collected from FM1-43-labelled astrocytes from A-SMase-wild type (+/+), heterozygous (+/−) or KO (−/−) mice. Astrocytes were exposed to 100 μM BzATP, recombinant (r-SMase) or bacterial (b-SMase) SMase, or a combination of BzATP and r-SMases/b-SMases (n of experimental sessions = 2; $P<0.01$, ANOVA analysis, Tukey's method). (**E**) ELISA evaluation of IL-1β levels in the supernatant of LPS-primed astrocytes exposed to 100 μM BzATP for 30 min, in the presence/absence of A-SMase inhibitors. Thirty minutes after BzATP addition, IL-1β is clearly detectable in vesicle-free supernatant fraction. $n = 3$; $P<0.01$, ANOVA analysis, Tukey's method. (**F**) ELISA for IL-1β on supernatant collected from BzATP-stimulated cortical astrocytes from A-SMase wild type (+/+), heterozygous (+/−) or KO (−/−) animals. BzATP-induced IL-1β release is completely blocked in KO cultures and partially rescued by addition of either r-SMase or b-SMase (n of experimental sessions = 2, $P<0.01$, ANOVA analysis, Tukey's method). Both r-SMase and b-SMase failed to induce IL-1β release in the absence of BzATP stimulation, confirming requirement of $P2X_7R$ activation for the cytokine processing and release (Sanz and Di Virgilio, 2000).

excluding that block of cytokine secretion depends on non-specific effects in A-SMase KO astrocytes. These data clearly indicate that A-SMase activity has an important function in IL-1β release by controlling $P2X_7$-dependent vesiculation.

Src kinase-dependent phosphorylation of p38 MAPK is involved in $P2X_7$-induced A-SMase activation

$P2X_7R$ is a ligand-gated ion channel, which induces the opening of large membrane pores, recently identified as pannexin-1 hemichannels (Pelegrin and Surprenant, 2006, 2007; Locovei *et al*, 2007). Independently of the molecular entity of the pore, several pieces of evidence indicate that $P2X_7$-induced pore formation requires activation of p38 MAPK cascade (Suzuki *et al*, 2004). We observed by western blotting that a brief BzATP exposure induces a prompt p38 MAPK phosphorylation in microglia (not shown) and cortical astrocytes (Figure 5A). p38 phosphorylation peaked 2–5 min after receptor stimulation and then slowly declined, being still above control levels 30 min after agonist addition. BzATP-induced p38 phosphorylation was prevented by the p38 specific inhibitor SB-203580 (400 nM, Figure 5B), by the kinase inhibitor genistein (50 μM, Figure 5B), and the *src*-kinase inhibitor PP2 (10 μM, not shown), indicating that p38 phosphorylation is mediated by an *src*-kinase family member, as suggested previously (Suzuki *et al*, 2004). BzATP-induced p38 activation was independent of the channel activity of the receptor, as it efficiently occurred also in the absence of extracellular Na^+ and Ca^{2+} and in the presence of high extracellular K^+ ions (Figure 5B). Consistent with the involvement of an *src*-family protein kinase in $P2X_7$-mediated p38 activation, exposure of astrocytes to BzATP in the presence of either PP2, genistein as well as SB203580 failed to induce pore opening, as assayed by YO-PRO-1 uptake (Figure 5C).

To evaluate whether $P2X_7$-mediated p38 phosphorylation and large pore formation could be relevant for A-SMase activation and vesiculation, A-SMase activity and MP shedding were analysed in microglial cells pre-treated with inhibitors of the p38 cascade. Inhibition of p38 strongly reduced A-SMase activity in microglia (Figure 5D) as well as the enzyme translocation to the PM (Figure 5E and F), thus indicating that A-SMase activation and membrane

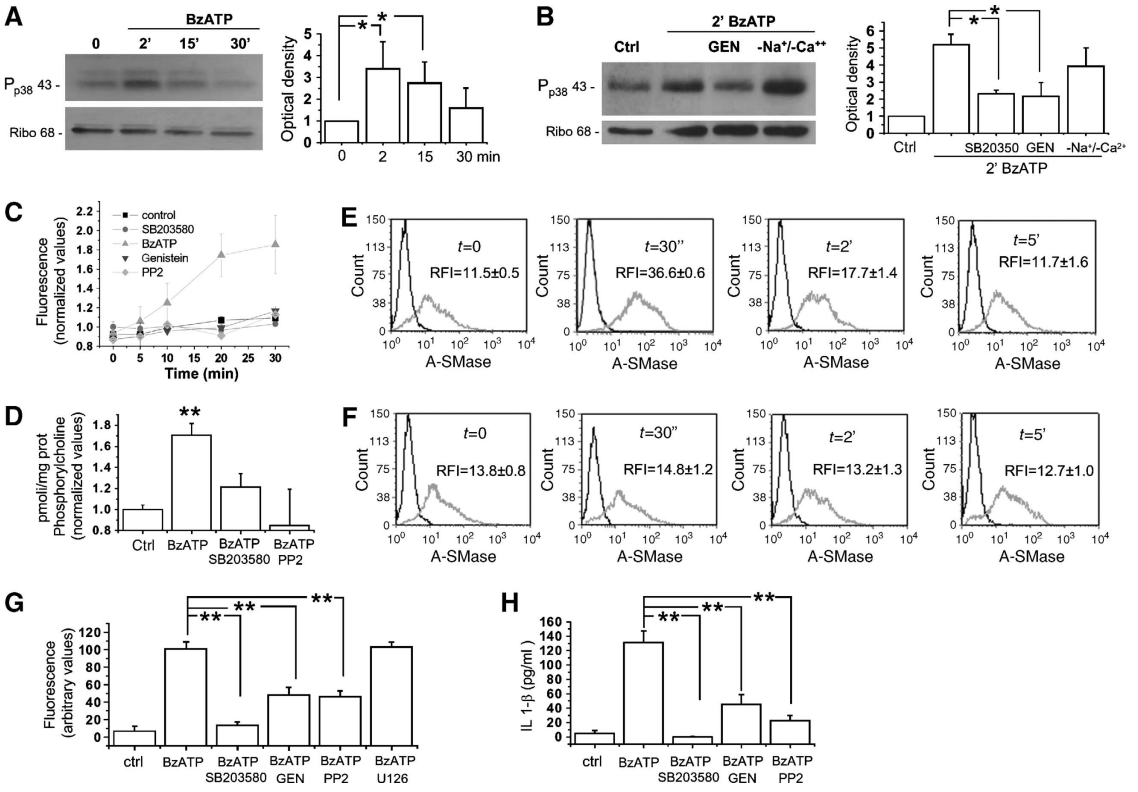

Figure 5 Src kinase-dependent phosphorylation of p38 MAPK mediates $P2X_7$-induced A-SMase activity. (**A**) Time course of p38 MAPK phosphorylation in astrocytes exposed to 100 μM BzATP for 2, 15 and 30 min. Right panel shows the quantitative analysis of P-p38 immunoreactivity normalised to ribophorin from three independent experiments. (**B**) Western blot analysis of cortical astrocytes exposed for 2 min to 100 μM BzATP in the presence/absence of the p38 MAPK inhibitor SB-203580 (400 nM) or the kinase inhibitor genistein (10 μM). Astrocytes were also exposed to BzATP in the absence of extracellular Na^+ and Ca^{2+} and high extracellular K^+ ions to inhibit ions influx. Right panel shows the quantitative analysis of P-p38 immunoreactivity normalised to the astrocyte marker ribophorin. (**C**) Time course analysis of Yo-PRO-1 uptake in astrocytes exposed to 100 μM BzATP in the absence or in the presence of the inhibitors of p38 MAPK phosphorylation pathway. Yo-PRO-1 uptake is sensitive to the inhibition p38 MAPK phosphorylation ($n=3$; $P<0.01$, ANOVA analysis, Dunnett's method). (**D**) A-SMase activity triggered by 100 μM BzATP treatment in the presence/absence of the p38 MAPK inhibitor SB-203580 (400 nM) or the *src*-kinase inhibitor PP2 (10 μM) ($n=3$; asterisks: $P<0.01$ versus control) normalised as described in Figure 3. (**E**, **F**) A-SMase exposure onto the PM induced by 100 μM BzATP treatment in the presence (E)/absence (F) of the p38 MAPK inhibitor SB-203580 (400 nM) measured by FACS in intact N9 microglial cells. The relative fluorescence intensity (RFI) was calculated versus negative controls. The results shown are from one experiment representative of three reproducible ones. The RFI values are determined as described in Figure 3. (**G**) Quantitative analysis of MPs pelleted at 10 000 *g* from the supernatants of FM1-43-labelled astrocytes exposed to 100 μM BzATP in the presence/absence of inhibitors of p38 MAPK phosphorylation pathway. FM1-43-labelled MPs pelleted at 10 000 *g* from the supernatants of astrocytes exposed to BzATP in the presence/absence of inhibitors of p38 MAPK phosphorylation pathway. (**H**) ELISA for IL-1β on supernatant conditioned for 30 min by 100 μM BzATP-stimulated astrocytes in the presence/absence of inhibitors of p38 MAPK phosphorylation pathway.

recruitment occur downstream of $P2X_7$-mediated p38 phosphorylation. As a consequence, MP shedding from either microglia (not shown) or cortical astrocytes (Figure 5G) pre-exposed to either SB-203580, genistein or PP2 was strongly reduced. No significant attenuation of MP shedding was induced by the ERK1/2 inhibitor U126 (10 μM) (Figure 5G). Moreover, IL-1β detection by ELISA on supernatants of astrocytes treated with SB-203580, PP2 or genistein revealed a strong reduction of cytokine release, thus indicating a clear involvement of p38 cascade in the process of cytokine release (Figure 5H).

We then investigated whether p38-dependent activation of A-SMase could be involved in $P2X_7$-induced pore formation. An efficient YO-PRO-1 uptake was observed in microglial pretreated with imipramine (Figure 6A; Supplementary data), indicating that A-SMase inhibition does not alter the capability of $P2X_7R$ to open large membrane pores. Accordingly, no significant differences in YO-PRO-1 uptake kinetics were detected in astrocytes from A-SMase KO and heterozygous mice as compared with astrocytes from wild-type animals (Figure 6B). These data suggest that MP shedding and pore opening are two $P2X_7$-dependent processes that are regulated by two parallel pathways, downstream of p38 phosphorylation (Figure 7).

Discussion

A-SMase is required for MP shedding in glial cells

In this study, we show that $P2X_7$-dependent shedding of PM-derived MPs is not restricted to microglia in the brain, as also astrocytes can shed MPs containing IL-1β. Glia-derived MPs present in the CNS, besides containing leaderless molecules relevant for neuroinflammation, could also represent a general mechanism used for signalling to other cells, such as neurons, through the intercellular transfer of protein/lipid components. All these reasons prompted us to further investigate the molecular mechanisms involved in glial MP formation and shedding.

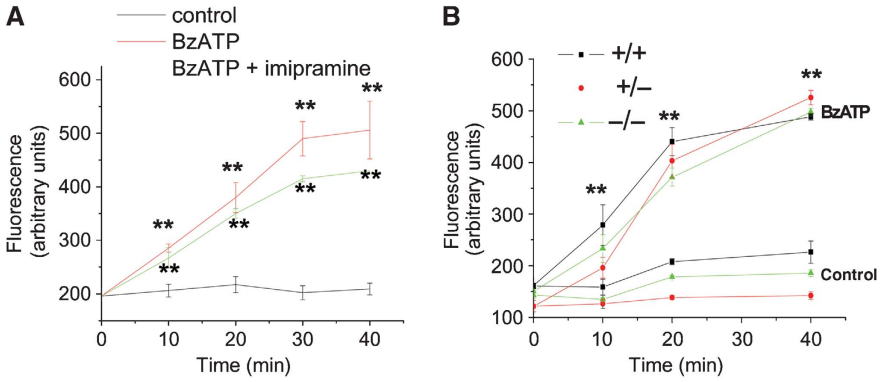

Figure 6 A-SMase activity does not control pore opening. (**A**) Time course analysis of Yo-PRO-1 uptake in astrocytes exposed to 100 μM BzATP in the presence/absence of A-SMase inhibitors. (**B**) Time course analysis of Yo-PRO-1 uptake in astrocytes from A-SMase wild type (+/+), heterozygous (+/−) or KO (−/−) animals on 100 μM BzATP exposure. ($n=2$; $^{**}P<0.01$ versus controls, ANOVA analysis, Dunnett's method).

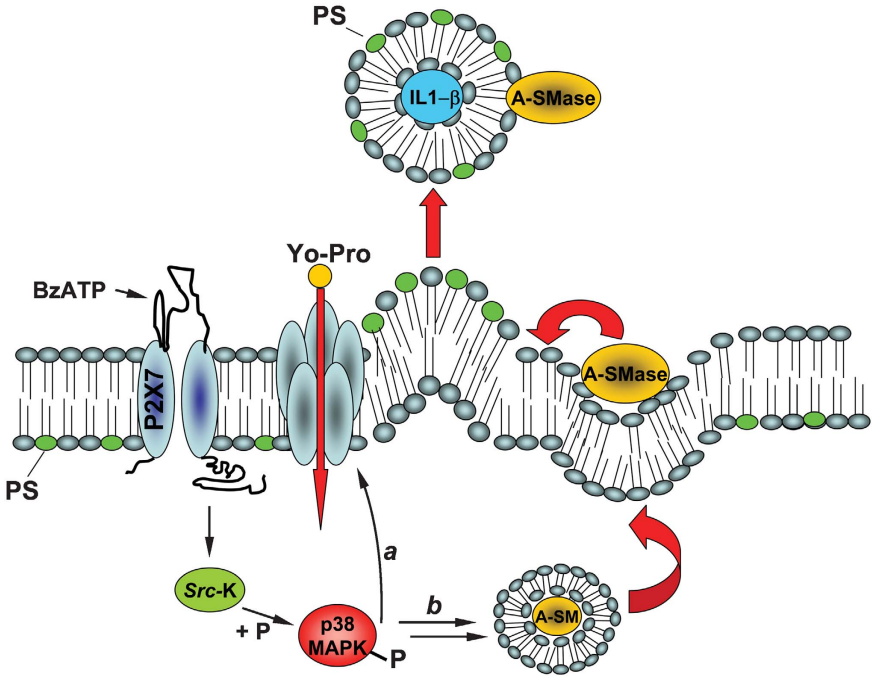

Figure 7 Model for $P2X_7R$-induced signalling pathway involved in MP shedding and large pore opening in glial cells. On BzATP stimulation, $P2X_7R$ activates p38 MAPK cascade through src kinase-mediated phosphorylation. In turn, P-p38 triggers different pathways, among which PM pore formation (a), and mobilisation of A-SMase from luminal lysosomal compartment to PM outer leaflet (b) where the enzyme alters membrane structure/fluidity leading to PM blebbing and shedding. Differently from exosomes, shed MPs carry IL-1β cytokine, present A-SMase and high levels of PS on their membrane outer leaflet and are 100–1000 nm in size.

Here, we show that budding and shedding of MPs is triggered by $P2X_7R$ stimulation that activates and recruits A-SMase. Of note, these results are consistent with previous evidence supporting a role of SMases in the budding of vesicles from microspheres (Nurminen *et al*, 2002), budding of exosomes into MVB (Trajkovic *et al*, 2008) and in apoptotic blebbing (Tepper *et al*, 2000), and with recent observation that $P2X_7R$ activation induces ceramide accumulation (Lepine *et al*, 2006). Both apoptotic blebbing and budding of exosomes into MVB result, however, from the activation of N- rather than A-SMase. The role of N-SMase in exosome release from oligodendrocytes (Trajkovic *et al*, 2008), together with the involvement of A-SMase in MP formation from glial cells (this study), indicate that different members of the SMase family specifically control the release of distinct populations of extracellular vesicles in the CNS.

Here, we provide evidence of a causal relationship between A-SMase activity and MP shedding and show that A-SMase is both sufficient and necessary for the shedding process in glial cells. First, A-SMase becomes promptly activated and translocated onto the PM on $P2X_7R$ stimulation, and the time course of its activation is consistent with that of MP shedding. Second, addition of exogenous r-SMase efficiently stimulates MP shedding, also in $P2X_7$-deficient microglia or in cells where the receptor activation is pharmacologically prevented. Finally, evidence obtained in cultures from KO mice indicates that absence of A-SMase completely abolishes MP release, which can be, however, rescued by

addition of exogenous r- or b-SMase. Although the complex changes in lipid storage and cholesterol trafficking consequent to A-SMase absence need further investigation, our results rule out the possibility that block of MP release may be caused by secondary non-specific problems of KO animals.

Up to 90% of SM is localised in the outer membrane leaflet (Koval and Pagano, 1991), thus, it is fully accessible for the enzyme shifted into the membrane. However, if SM is hydrolyzed extracellularly, ceramide has to redistribute within the lipid bilayer, as clustering of ceramide into the inner leaflet, due to the spontaneous negative curvature of the lipid, can facilitate formation of PM protrusions (Goni and Alonso, 2006). Previous studies have shown that A-SMase may have an extracellular action, as showed by the enzyme secretion and the capability to move onto the cell surface in response to such stimuli such as CD95 or Pseudomonas aeruginosa infection (Grassmé *et al*, 2001). Enrichment of A-SMase in MPs suggests that formation of membrane protrusions occurs from specific PM domains, the so-called lipid rafts, where accumulation of ceramide by local translocation of A-SMase can promote the enlargement of these domains (Garcia-Marcos *et al*, 2006) and facilitate membrane blebbing. In such domains, cytoskeleton/membrane proteins, possibly directly interacting with the $P2X_7R$- and $P2X_7R$-dependent signalling components, could be recruited. Interestingly, a domain analogous to the TNFR1 death domain has been described in the C-terminus of the $P2X_7R$, which could target the receptor to lipid rafts.

$P2X_7$-induced signalling pathway of MP shedding

This study provides novel insights into the signalling pathway downstream of $P2X_7Rs$, which regulates MP shedding in glial cells. Our data support a model (Figure 7) in which, among the multiple intracellular signals coupled to $P2X_7R$, p38 MAPK cascade is required for the shedding process; indeed we found that P38 becomes promptly phosphorylated on $P2X_7R$ activation, also in the absence of extracellular Na^+ and Ca^{2+} and in high extracellular K^+, indicating that $P2X_7R$ regulates p38 activation by a metabotropic pathway independent of the channel function of the receptor. Inhibition of p38 phosphorylation by PP2 indicates the involvement of an *src*-protein tyrosine kinase as a link between $P2X_7R$ and p38, as also suggested by Suzuki *et al* (2004). The Src homology 3 (SH3) domains of these soluble kinases may well interact with the SH3-binding motif present in the C-terminus of the $P2X_7R$ (Denlinger *et al*, 2001). P-p38 induces translocation of endogenous A-SMase into the outer membrane leaflet and stimulates the enzyme activity, thus, inducing SM breakdown and ceramide generation. Although how P-p38 can induce A-SMase translocation and activation remains to be completely elucidated, our data clearly indicate that P-p38 acts upstream of A-SMase activity.

$P2X_7$-induced vesicle shedding and large pore opening

So far controversial results have been published concerning $P2X_7$-dependent p38 activation, opening of large membrane pores and release of IL-1β. In THP-1 monocytes, p38 inhibition does not alter IL-1β release although it inhibits large pore opening (Donnelly-Roberts *et al*, 2004). Inhibition of pore formation by p38 blockers has also been reported in peritoneal macrophages (Faria *et al*, 2005), whereas no effect has been detected in peripheral macrophages (Da Cruz *et al*, 2006). Our data indicate that YO-PRO uptake is blocked by agents that interfere with p38 cascade, downstream of $P2X_7R$. Recently, the large pore that opens on $P2X_7R$ activation has been identified with pannexin-1, a membrane protein that forms gap junctions when expressed in oocytes and epithelial cells. Blockade of pannexin-1 abolishes caspase-1 processing and IL-1β release, thus, indicating a role of pannexin-1 in cytokine processing and secretion (Pelegrin and Surprenant, 2006, 2007). However, $P2X_7R$-mediated, pannexin-1-dependent dye uptake is unlikely responsible for caspase-1 activation and IL-1β processing, because dye uptake occurs in high extracellular K^+, when IL-1β release is abrogated (Pelegrin and Surprenant, 2007). Our finding that A-SMase inhibitors and genetic deficiency of A-SMase do not affect the ability of the $P2X_7R$ to induce dye uptake, while strongly inhibiting the cytokine release, further confirms that pore opening is not directly involved in IL-1β processing and release. Pore opening and IL-1β release through MP shedding are, in fact, two parallel events occurring downstream of $P2X_7R$-dependent p38 phosphorylation (Figure 7). Furthermore, although $P2X_7R$-dependent p38 phosphorylation (this study) and blebbing do not require ion influx through the receptor, extracellular Ca^{2+} is necessary for MP shedding (MacKenzie *et al*, 2001; Bianco *et al*, 2005) and processing of IL-1β, at least in some cell types as microglia and monocytes (Brough *et al*, 2003; Gudipaty *et al*, 2003).

Imipramine, an old drug for inhibiting IL-1β release in brain pathologies?

Other pathways besides MP shedding have been proposed to mediate IL-1β release from monocytes/macrophages, including exocytosis of secretory lysosomes and exosomes (Andrei *et al*, 1999; Qu *et al*, 2007). Complete blockade of MP shedding and IL-1β release from A-SMase KO astrocytes indicates that release of MPs from PM represents the major mechanism mediating secretion of the cytokine from glial cells. Concerning the possible contribution of secretory lysosomes, although it has been recently reported that IL-1β release is not affected in macrophages isolated from mice carrying a mutated Lyst gene, which have impaired lysosomal secretion (Brough and Rothwell, 2007), our results do not allow to exclude the contribution of these organelles to the cytokine release.

Consistent with the role of A-SMase in IL-1β secretion, reduced levels of IL-1β have been reported in the brain of A-SMase KO mice (Ng and Griffin, 2006), although A-SMase might not be necessary for the cytokine release outside the nervous system (Grassmé *et al*, 2003). Under this respect it might be tempting to speculate that the increased frequency of infections observed both in A-SMase KO animals and in patient affected with Niemann Pick type A and B diseases (Minai *et al*, 2000; Ikegami *et al*, 2003) might be related with the capability of A-SMase to control cytokine release (Leventhal *et al*, 2001) and consequently to regulate the immune responses. A-SMase can, therefore, represent a new suitable target for the pharmacological treatment of pathologies, like multiple sclerosis (MS), where IL-1β is implicated. Previous studies have described that interference with the IL-1β-mediated inflammatory pathway has a positive outcome in experimental autoimmune encephalomyelitis (EAE) mice, a well-characterised model of MS (Martin and Near, 1995; Wiemann *et al*, 1998; Furlan *et al*, 1999). Interestingly, the antidepressant drug imipramine, besides improving depression symptoms (Pollak *et al*, 2002), was

found to reduce EAE-mice mortality and body weight loss. Our study, showing that imipramine, which is also a A-SMase inhibitor, blocks release of IL-1β vesicles by hampering A-SMase mediated MP shedding, defines the possible molecular mechanisms underlying previous observations in EAE-mice. Given that the efficacy of current therapies for MS is rather limited and is mainly aimed at slowing the progression of the disease, the present identification of imipramine, a widely used tricyclic antidepressant, as a potent blocker of IL-1β release could be of great relevance as a starting point to identify more efficacious drugs for the pharmacological treatment for this pathology.

Materials and methods

Cell cultures and cell stimulation

Glial cells were obtained and maintained as described previously (Calegari *et al*, 1999; Bianco *et al*, 2005). Human glioblastoma cell line ADF was obtained from PG Natali (Istituto Regina Elena, Rome, Italy) and cultured as described in Supplementary data. For induction of PM-derived MPs see Supplementary data.

Vesicle isolation by differential centrifugation

Isolation of vesicle populations by differential centrifugation was implemented from a previous paper (Marzesco *et al*, 2005), as described in Supplementary data.

Quantification of PM-derived MPs

Spectrophotometric quantification of FM1-43-labelled MPs was carried out in KRH devoid of BSA as described previously (Supplementary data; Bianco *et al*, 2005).

Fluorescence microscopy of vesicles

P2, P3 and P4 pellets were obtained from BzATP-stimulated, confluent astrocytes or N9 cells by differential centrifugation and stained as described in Supplementary data.

FACS analysis

P2, P3 and P4 pellets were obtained from BzATP-stimulated, confluent astrocytes (24×10^6 cells) or confluent N9 cells (42×10^6 cells) by differential centrifugation and analysed as described in Supplementary data by a FacsCalibur flow cytometer (Becton Dickinson). Analysis of surface A-SMase in intact cells by FACS was carried out as described in Supplementary data.

A-SMase cell surface labelling and immunoprecipitation

Analysis of A-SMase cell surface exposure was carried out by biotinylation and subsequent western blotting as described in Supplementary data.

Electron microscopy of vesicles

P2, P3 and P4 pellets from BzATP-stimulated astrocytes or N9 cells were fixed with 4% paraformaldehyde in PBS for 12 h at 4°C and processed for negative staining electron microscopy (Supplementary data).

Measurement of A-SMase activity

A-SMase activity was determined as described previously (Falcone *et al*, 2004).

IL-1β ELISA

Cells were primed for 6 h with 100 ng/ml LPS. A mouse IL-1β ELISA kit (Pierce Endogen, Italy) was used to quantify the presence of IL-1β in the supernatant of astrocytes and microglia cells stimulated with 100 μM BzATP.

Chemicals and antibodies

For chemicals see Supplementary data. Rabbit Ab versus ribophorin (1:2000) were kindly provided by Dr Kreibich (New York University, New York, NY, USA). Mouse Ab versus Na^+/K^+ ATPase (1:5000) and rabbit Ab versus GLAST N-epitope (1:150) were provided by Dr Pietrini, University of Milan, Italy. Rabbit Ab versus P-p38 MAPK (1:400) was from Cell Signalling Technology (USA) and goat Ab versus IL-1β (1:1000) was from R&D (USA). The anti-A-SMase rabbit polyclonal Ab (1:500) was generated in the lab and described in Perrotta *et al* (2007). Example of specificity of this Ab in western blotting is shown in Supplementary Figure 4. Mouse monoclonal anti-HSP70 Ab (BRM-22 clone, 1:1000) and mouse monoclonal GFAP Ab (G-A-5 clone, 1:1000) were from Sigma. Goat polyclonal anti-CD63/LAMP3 Ab (clone M-13, 1:50) was from Santa Cruz Biotech. Rabbit polyclonal anti-Cathepsin B Ab (1:200) was from Chemicon. Rabbit polyclonal anti-CB1 Ab (1:500) was kindly provided by Dr Mackie, University of Washington, Seattle, USA.

Statistical analysis

All data are presented as means ± s.e. from the indicated number of experiments. Statistical significance was evaluated using either Student's *t*-test or one-way ANOVA analysis of variance. The differences were considered to be significant if $P<0.05$ and are indicated by an asterisk; those at $P<0.01$ are indicated by double asterisks.

Supplementary data

Supplementary data are available at *The EMBO Journal* Online (http://www.embojournal.org).

Acknowledgements

We thank A Colombo and G Biella (University of Milano, Italy) for help in some experiments; Dr F Di Virgilio (University of Ferrara, Italy) for the $P2X_7$-deficient N9 microglial clone; Dr M Canossa (University of Bologna, Italy) and Dr L Galli-Resta (CNR Institute of Neuroscience, Pisa, Italy) for helpful comments and discussion. This work was supported by FISM (2007/R35) to CV, CARIPLO 20060948 and EU-Synapse Integrated Project (LSHM-CT-2005-019055) to MM and AIRC (Italian Cancer Association) to EC. CP is recipient of an AIRC fellowship. Research in EHS lab was supported by NIH grant R01HD28607. Grant S Paolo 2500.1964.

References

Andrei C, Dazzi C, Lotti L, Torrisi MR, Chimini G, Rubartelli A (1999) The secretory route of the leaderless protein interleukin 1beta involves exocytosis of endolysosome-related vesicles. *Mol Biol Cell* **10:** 1463–1475

Bianco F, Pravettoni E, Colombo A, Schenk U, Moller T, Matteoli M, Verderio C (2005) Astrocyte-derived ATP induces vesicle shedding and IL-1 beta release from microglia. *J Immunol* **174:** 7268–7277

Brough D, Le Feuvre RA, Wheeler RD, Solovyova N, Hilfiker S, Rothwell NJ, Verkhratsky A (2003) Ca2 + stores and Ca2 + entry differentially contribute to the release of IL-1 beta and IL-1 alpha from murine macrophages. *J Immunol* **170:** 3029–3036

Brough D, Rothwell NJ (2007) Caspase-1-dependent processing of pro-interleukin-1beta is cytosolic and precedes cell death. *J Cell Sci* **120:** 772–781

Calegari F, Coco S, Taverna E, Bassetti M, Verderio C, Corradi N, Matteoli M, Rosa P (1999) A regulated secretory pathway in cultured hippocampal astrocytes. *J Biol Chem* **274:** 22539–22547

Chang CP, Zhao J, Wiedmer T, Sims PJ (1993) Contribution of platelet microparticle formation and granule secretion to the transmembrane migration of phosphatidylserine. *J Biol Chem* **268:** 7171–7178

Coleman ML, Sahai EA, Yeo M, Bosch M, Dewar A, Olson MF (2001) Membrane blebbing during apoptosis results from caspase-mediated activation of ROCK I. *Nat Cell Biol* **3:** 339–345

da Cruz CM, Ventura AL, Schachter J, Costa-Junior HM, da Silva Souza HA, Gomes FR, Coutinho-Silva R, Ojcius DM, Persechini PM (2006) Activation of ERK1/2 by extracellular nucleotides in macrophages is mediated by multiple P2 receptors independently of P2X7-associated pore or channel formation. *Br J Pharmacol* **147:** 324–334

Denlinger LC, Fisette PL, Sommer JA, Watters JJ, Prabhu U, Dubyak GR, Proctor RA, Bertics PJ (2001) Cutting edge: the nucleotide receptor P2X7 contains multiple protein- and lipid-interaction motifs including a potential binding site for bacterial lipopolysaccharide. *J Immunol* **167:** 1871–1876

Donnelly-Roberts DL, Namovic MT, Faltynek CR, Jarvis MF (2004) Mitogen-activated protein kinase and caspase signaling pathways are required for P2X7 receptor (P2X7R)-induced pore formation in human THP-1 cells. *J Pharmacol Exp Ther* **308:** 1053–1061

Duan S, Neary JT (2006) P2X(7) receptors: properties and relevance to CNS function. *Glia* **54:** 738–746

Falcone S, Perrotta C, De Palma C, Pisconti A, Sciorati C, Capobianco A, Rovere-Querini P, Manfredi AA, Clementi E (2004) Activation of acid sphingomyelinase and its inhibition by the nitric oxide/cyclic guanosine 3′,5′-monophosphate pathway: key events in Escherichia coli-elicited apoptosis of dendritic cells. *J Immunol* **173:** 4452–4463

Faria RX, Defarias FP, Alves LA (2005) Are second messengers crucial for opening the pore associated with P2X7 receptor? *Am J Physiol Cell Physiol* **288:** 260–271

Fauré J, Lachenal G, Court M, Hirrlinger J, Chatellard-Causse C, Blot B, Grange J, Schoehn G, Goldberg Y, Boyer V, Kirchhoff F, Raposo G, Garin J, Sadoul R (2006) Exosomes are released by cultured cortical neurones. *Mol Cell Neurosci* **4:** 642–648

Ferrari D, Chiozzi P, Falzoni S, Dal Susino M, Collo G, Buell G, Di Virgilio F (1997) ATP-mediated cytotoxicity in microglial cells. *Neuropharmacology* **9:** 1295–1301

Furlan R, Martino G, Galbiati F, Poliani PL, Smiroldo S, Bergami A, Desina G, Comi G, Flavell R, Su MS, Adorini L (1999) Caspase-1 regulates the inflammatory process leading to autoimmune demyelination. *J Immunol* **163:** 2403–2409

Garcia-Marcos M, Pochet S, Marino A, Dehaye JP (2006) P2X7 and phospholipid signalling: the search of the ''missing link'' in epithelial cells. *Cell Signal* **18:** 2098–2104

Goni FM, Alonso A (2006) Biophysics of sphingolipids I. Membrane properties of sphingosine, ceramides and other simple sphingolipids. *Biochim Biophys Acta* **1758:** 1902–1921

Grassmé H, Jekle A, Riehle A, Schwarz H, Berger J, Sandhoff K, Kolesnick R, Gulbins E (2001) CD95 signaling via ceramide-rich membrane rafts. *J Biol Chem* **276:** 20589–20596

Grassmé H, Jendrossek V, Riehle A, von Kürthy G, Berger J, Schwarz H, Weller M, Kolesnick R, Gulbins E (2003) Host defense against Pseudomonas aeruginosa requires ceramide-rich membrane rafts. *Nat Med* **9:** 322–330

Gudipaty L, Munetz J, Verhoef PA, Dubyak GR (2003) Essential role for Ca2 + in regulation of IL-1beta secretion by P2X7 nucleotide receptor in monocytes, macrophages, and HEK-293 cells. *Am J Physiol Cell Physiol* **285:** 286–299

Gulbins E, Jekle A, Ferlinz K, Grassmé H, Lang F (2000) Physiology of apoptosis. *Am J Physiol Renal Physiol* **4:** 605–615

Gulbins E (2003) Regulation of death receptor signaling and apoptosis by ceramide. *Pharmacol Res* **47:** 393–399

Heijnen HF, Schiel AE, Fijnheer R, Geuze HJ, Sixma JJ (1999) Activated platelets release two types of membrane vesicles: microvesicles by surface shedding and exosomes derived from exocytosis of multivesicular bodies and alpha-granules. *Blood* **11:** 3791–3799

Ikegami M, Dhami R, Schuchman EH (2003) Alveolar lipoproteinosis in an acid sphingomyelinase-deficient mouse model of Niemann-Pick disease. *Am J Physiol Lung Cell Mol Physiol* **284:** 518–525

Koval M, Pagano RE (1991) Intracellular transport and metabolism of sphingomyelin. *Biochim Biophys Acta* **1082:** 113–125

Lepine S, Le Stunff H, Lakatos B, Sulpice JC, Giraud F (2006) ATP-induced apoptosis of thymocytes is mediated by activation of P2 X 7 receptor and involves *de novo* ceramide synthesis and mitochondria. *Biochim Biophys Acta* **1761:** 73–82

Leventhal AR, Chen W, Tall AR, Tabas I (2001) Acid sphingomyelinase-deficient macrophages have defective cholesterol trafficking and efflux. *J Biol Chem* **276:** 44976–44983

Locovei S, Scemes E, Qiu F, Spray DC, Dahl G (2007) Pannexin1 is part of the pore forming unit of the P2X(7) receptor death complex. *FEBS Lett* **581:** 483–488

MacKenzie A, Wilson HL, Kiss-Toth E, Dower SK, North RA, Surprenant A (2001) Rapid secretion of interleukin-1beta by microvesicle shedding. *Immunity* **15:** 825–835

Marchesini N, Hannun YA (2004) Acid and neutral sphingomyelinases: roles and mechanisms of regulation. *Biochem Cell Biol* **82:** 27–44

Martin D, Near SL (1995) Protective effect of the interleukin-1 receptor antagonist (IL-1ra) on experimental allergic encephalomyelitis in rats. *J Neuroimmunol* **61:** 241–245

Marty V, Médina C, Combe C, Parnet P, Amédée T (2005) ATP binding cassette transporter ABC1 is required for the release of interleukin-1beta by P2X7-stimulated and lipopolysaccharide-primed mouse Schwann cells. *Glia* **49:** 511–519

Marzesco AM, Janich P, Wilsch-Brauninger M, Dubreuil V, Langenfeld K, Corbeil D, Huttner WB (2005) Release of extracellular membrane particles carrying the stem cell marker prominin-1 (CD133) from neural progenitors and other epithelial cells. *J Cell Sci* **118:** 2849–2858

Minai OA, Sullivan EJ, Stoller JK (2000) Pulmonary involvement in Niemann-Pick disease: case report and literature review. *Respir Med* **12:** 1241–1251

Morelli A, Chiozzi P, Chiesa A, Ferrari D, Sanz JM, Falzoni S, Pinton P, Rizzuto R, Olson MF, Di Virgilio F (2003) Extracellular ATP causes ROCK I-dependent bleb formation in P2X7-transfected HEK293 cells. *Mol Biol Cell* **14:** 2655–2664

Morelli AE, Larregina AT, Shufesky WJ, Sullivan ML, Stolz DB, Papworth GD, Zahorchak AF, Logar AJ, Wang Z, Watkins SC, Falo Jr LD, Thomson AW (2004) Endocytosis, intracellular sorting, and processing of exosomes by dendritic cells. *Blood* **104:** 3257–3266

Nedergaard M, Ransom B, Goldman SA (2003) New roles for astrocytes: redefining the functional architecture of the brain. *Trends Neurosci* **10:** 523–530

Neufeld EB, Cooney AM, Pitha J, Dawidowicz EA, Dwyer NK, Pentchev PG, Blanchette-Mackie EJ (1996) Intracellular trafficking of cholesterol monitored with a cyclodextrin. *J Biol Chem* **271:** 21604–21613

Ng CG, Griffin DE (2006) Acid sphingomyelinase deficiency increases susceptibility to fatal alphavirus encephalomyelitis. *J Virol* **80:** 10989–10999

Nurminen TA, Holopainen JM, Zhao H, Kinnunen PK (2002) Observation of topical catalysis by sphingomyelinase coupled to microspheres. *J Am Chem Soc* **124:** 12129–12134

Pelegrin P, Surprenant A (2006) Pannexin-1 mediates large pore formation and interleukin-1beta release by the ATP-gated P2X7 receptor. *EMBO J* **25:** 5071–5082

Pelegrin P, Surprenant A (2007) Pannexin-1 couples to maitotoxin- and nigericin-induced interleukin-1beta release through a dye uptake-independent pathway. *J Biol Chem* **282:** 2386–2394

Perrotta C, Bizzozero L, Falcone S, Rovere-Querini P, Prinetti A, Schuchman EH, Sonnino S, Manfredi AA, Clementi E (2007) Nitric oxide boosts chemoimmunotherapy via inhibition of acid sphingomyelinase in a mouse model of melanoma. *Cancer Res* **67:** 7559–7564

Pollak Y, Orion E, Goshen I, Ovadia H, Yirmiya R (2002) Experimental autoimmune encephalomyelitis-associated behavioral syndrome as a model of 'depression due to multiple sclerosis'. *Brain Behav Immun* **16:** 533–543

Potolicchio I, Carven GJ, Xu X, Stipp C, Riese RJ, Stern LJ, Santambrogio L (2005) Proteomic analysis of microglia-derived exosomes: metabolic role of the aminopeptidase CD13 in neuropeptide catabolism. *J Immunol* **4:** 2237–2243

Qu Y, Franchi L, Nunez G, Dubyak GR (2007) Nonclassical IL-1 beta secretion stimulated by P2X7 receptors is dependent on inflammasome activation and correlated with exosome release in murine macrophages. *J Immunol* **179:** 1913–1925

Ratajczak J, Wysoczynski M, Hayek F, Janowska-Wieczorek A, Ratajczak MZ (2006) Membrane-derived microvesicles: important and underappreciated mediators of cell-to-cell communication. *Leukemia* **20:** 1487–1495

Sanz JM, Di Virgilio F (2000) Kinetics and mechanism of ATP-dependent IL-1 beta release from microglial cells. *J Immunol* **164:** 4893–4898

Schiera G, Proia P, Alberti C, Mineo M, Savettieri G, Di Liegro I (2007) Neurons produce FGF2 and VEGF and secrete them at least in part by shedding extracellular vesicles. *J Cell Mol Med* **6:** 1384–1394

Simons K, Ikonen E (1997) Functional rafts in cell membranes. *Nature* **387:** 569–572

Simpson RJ, Jensen SS, Lim JW (2008) Proteomic profiling of exosomes: current perspectives. *Proteomics* **19:** 4083–4099

Slotte JP, Hedstrom G, Rannstrom S, Ekman S (1989) Effects of sphingomyelin degradation on cell cholesterol oxidizability and steady-state distribution between the cell surface and the cell interior. *Biochim Biophys Acta* **985:** 90–96

Smalheiser NR (2007) Exosomal transfer of proteins and RNAs at synapses in the nervous system. *Biol Direct* **2:** 35

Suzuki T, Hide I, Ido K, Kohsaka S, Inoue K, Nakata Y (2004) Production and release of neuroprotective tumor necrosis factor by P2X7 receptor-activated microglia. *J Neurosci* **24:** 1–7

Taylor AR, Robinson MB, Gifondorwa DJ, Tytell M, Milligan CE (2007) Regulation of heat shock protein 70 release in astrocytes: role of signaling kinases. *Dev Neurobiol* **13:** 1815–1829

Tepper AD, Ruurs P, Wiedmer T, Sims PJ, Borst J, van Blitterswijk WJ (2000) Sphingomyelin hydrolysis to ceramide during the execution phase of apoptosis results from phospholipid scrambling and alters cell-surface morphology. *J Cell Biol* **150:** 155–164

Théry C, Boussac M, Véron P, Ricciardi-Castagnoli P, Raposo G, Garin J, Amigorena S (2001) Proteomic analysis of dendritic cell-derived exosomes: a secreted subcellular compartment distinct from apoptotic vesicles. *J Immunol* **166:** 7309–7318

Trajkovic K, Hsu C, Chiantia S, Rajendran L, Wenzel D, Wieland F, Schwille P, Brugger B, Simons M (2008) Ceramide triggers budding of exosome vesicles into multivesicular endosomes. *Science* **319:** 1244–1247

Van Blitterswijk WJ, De Veer G, Krol JH, Emmelot P (1982) Comparative lipid analysis of purified plasma membranes and shed extracellular membrane vesicles from normal murine thymocytes and leukemic GRSL cells. *Biochim Biophys Acta* **688:** 495–504

Verhoef PA, Estacion M, Schilling W, Dubyak GR (2003) P2X7 receptor-dependent blebbing and the activation of Rho-effector kinases, caspases, and IL-1 beta release. *J Immunol* **170:** 5728–5738

Wiemann B, Van GY, Danilenko DM, Yan Q, Matheson C, Munyakazi L, Ogenstad S, Starnes CO (1998) Combined treatment of acute EAE in Lewis rats with TNF-binding protein and interleukin-1 receptor antagonist. *Exp Neurol* **149:** 455–463

